A combined spectroscopic and theoretical approach to investigate structural properties of Co(II)/Co(III) tris-cysteinato complexes in aqueous medium†

Carole Bresson,*[a] Riccardo Spezia,*[b] Stéphane Esnouf,[c] Pier Lorenzo Solari,[d] Stéphanie Coantic[e] and Christophe Den Auwer[f]

Received (in Montpellier, France) 9th May 2007, Accepted 11th June 2007
First published as an Advance Article on the web 28th June 2007
DOI: 10.1039/b707055a

Physiological and toxicological effects of metallic ions depend on their speciation and on the structure of their associated bioligand complexes. In the field of chemical and/or nuclear toxicological studies, we are investigating cobalt complexes with biorelevant ligands such as amino acids or peptides. The aqueous reaction of cobalt dichloride with an excess of cysteine (Cys, $C_3H_5NSO_2^{2-}$) in a basic medium under an anaerobic atmosphere and subsequent oxidation by O_2, afforded the mononuclear complexes Co(II):3Cys and Co(III):3Cys, respectively. A combination of X-ray absorption spectroscopy (XAS) measurements and Car-Parrinello molecular dynamics (CPMD) simulations allowed us to assess structural features of the already explored Co(III):3Cys complex. Inclusion of the temperature effects in the CPMD calculations gives an implicit access to disorder effects in the extended X-ray absorption fine structure (EXAFS) equation. The very good agreement between the measured and the simulated data showed the accuracy of these models provided by CPMD. The present investigation is completed by new UV-visible, X-ray absorption near edge structure (XANES) and electron paramagnetic resonance (EPR) data of Co(II):3Cys. These data are consistent with a Co(II) high-spin d^7 complex in a distorted octahedral geometry. This work contributes to the knowledge of topics such as metal–bioligand interaction which is of major interest in the field of bioinorganic chemistry.

Introduction

The study of interactions between metallic ions and biological macromolecules is one of the main interests in bioinorganic chemistry since most of the important biochemical processes involve the participation of metal-containing proteins.[1] In order to unveil the nature of activity and/or function of transition metals in biological systems, it is essential to gain knowledge of the molecular geometries of the metallic centres in the different metallobiomolecules.[2] Such information can be obtained through structural and spectroscopic investigations of model complexes containing relatively simple building blocks like amino acids or peptides.[3]

Among the various transition metals that are involved in biological processes, the cobalt cation is of major interest. At low concentrations, cobalt is a biologically essential trace element for humans.[4] However, cobalt may be toxic at high concentrations, leading to adverse health effects.[5] Of particular radio- or toxicological concern is, for example, the case of skin contamination with ^{60}Co of workers exposed to specific occupational conditions in the nuclear industry.[6] Indeed ^{59}Co, the natural stable isotope of cobalt, is present in alloys in nuclear power plants and its activation by thermal neutrons produces ^{60}Co. This isotope is of particular importance because of its long half-life (5.3 years) and its high energy emission of gamma photons. Attention has also been paid to ^{60}Co due to its presence in radioactive waste discharges, which can represent biogeochemical problems.[7] In the case of individual contamination, the nature of the chemical forms of cobalt that are present *in vivo*, as well as the molecular bases of its toxicity, transport, accumulation or detoxification, are far from being understood.[8] In order to elucidate these phenomena, as well as to understand the biological role and functions of cobalt and its potential radiological impact, preliminary structural investigations of cobalt complexes containing biorelevant ligands are of great interest.

Among the different spectroscopic techniques that can directly probe the environment of the metallic cations, XAS has long been widely and successfully applied to inorganic or bioinorganic systems, such as metalloproteins,[9] because of its

[a] *CEA Saclay, DEN/DPC/SECR/LSRM, 91191 Gif sur Yvette, France. E-mail: carole.bresson@cea.fr; Fax: +33 1 690 854 11; Tel: +33 1 690 883 48*
[b] *LAMBE, UMR CNRS 8587, Université d'Evry-Val-d'Essonne, 91025 Evry Cedex, France. E-mail: riccardo.spezia@univ-evry.fr; Fax: +33 1 694 776 55; Tel: +33 1 694 776 53*
[c] *Ecole Polytechnique, DSM/DRECAM/LSI, 91128 Palaiseau Cedex, France*
[d] *Synchrotron Soleil, Saint Aubin - BP 48, 91192 Gif-sur-Yvette Cedex, France*
[e] *ICSM, FRE CEA/CNRS 2926, CEA Valrhô/DRCP/SCPS/LCAM, BP 17171, 30207 Bagnols sur Cèze Cedex, France*
[f] *CEA Marcoule, DEN/DRCP/SCPS, 30207 Bagnols sur Cèze Cedex, France*
† The HTML version of this article has been enhanced with colour images.

element specificity[10] and its insensitivity to the physical state of the sample. This technique is based on data fitting to a proposed model structure, established with spectroscopic and structural techniques and based on the same or related systems. Hence, the availability of suitable starting models is a crucial point for data analysis. Among the possible models that can be used, molecular models based on theoretical chemical calculations have gained increasing interest as they can provide adequate *in silico* model compounds. Indeed, theoretical calculations have proved to be a crucial tool to suggest geometric and electronic structures of metallic complexes.[11] Adjustment of the EXAFS signal using computational methods is sometimes performed using classical molecular dynamics (MD),[12] which can provide model clusters including solvent effects and afford implicit access to Debye–Waller factors.[13] While classical MD can span long time scales (from ns to μs), allowing information on reactivity to be obtained, this approach suffers the limitation of the *a priori* knowledge of key interaction strength of the studied system (here the metal–ligands interaction). This limitation can be overcome by making use of Car-Parrinello molecular dynamics (CPMD).[14] This approach—based on density functional theory (DFT)—is able to give information on both the chemistry and the dynamical properties of a given system (temperature and environmental effects, *i.e.* structural disorder). These simulations can be applied to gas,[15] liquid[16] and solid[17] phases. In the field of bioinorganic chemistry, recent significant research efforts have been devoted to obtain a better insight into processes occurring in proteins' active sites by studying elaborated model complexes by theoretical approaches.[18] However, at the moment, CPMD simulations are limited in the time length available (ps timescales are accessible in condensed phase for such complex systems). This is an original combination of CPMD calculations with EXAFS data analysis that we present here.

Among the twenty natural occurring amino acids, cysteine can be considered as one of the most biorelevant since its thiol function confers to this ligand unique and important properties in protein structure, enzymatic activity and as a detoxifying agent in the human body.[19] This is the reason that prompted us to study mononuclear bis and tris Co(III)-cysteinato complexes ($[Co(Cys)_2(H_2O)_2]^{2-}$ and $[Co(Cys)_3]^{3-}$, respectively) mainly by X-ray absorption spectroscopy, as documented in our previous paper.[20] The description of the cobalt coordination sphere in $[Co(III)(Cys)_3]^{3-}$, obtained by the combination of EXAFS and CPMD, is compared to those proposed previously[20] using a more classical approach of EXAFS data fitting.

While Co(III)-cysteinato complexes have also been the subject of previous spectrophotometric, NMR and circular dichroism studies,[21] little attention has been paid up to now to Co(II)-cysteinato complexes. The investigation of Co(II) coordination with N and S ligands as well as the study of the reaction of the corresponding complexes with molecular oxygen are of relevance regarding living media since different oxidation states of the same metallic ion could be involved in *in vivo* biochemical processes. Hence, as we report in this paper, by using an original combination of CPMD calculations with EXAFS data, we have investigated the *in situ* oxidation of the new Co(II) tris-cysteinato complex by O_2. To the best of our knowledge, no specific interaction potentials (*i.e.* non-transferable or few-transferable) have been reported for cobalt–cysteine systems. UV-visible, EPR and XANES features complementary describe the electronic state of cobalt upon the oxidation process from Co(II) into Co(III).

Experimental

Sample preparation

Ex situ Co(III):3Cys was obtained as described in our previous paper.[20] Co(II):3Cys was prepared in the same manner except that the synthesis was carried out under an anaerobic atmosphere, leading to a blue purple complex. Monitoring of *in situ* oxidation of Co(II):3Cys was carried out independently. Co(II):3Cys was prepared in a first step and then exposed to air to oxidize Co(II) into Co(III), giving Co(III):3Cys.

UV-vis spectroscopy

The electronic spectra of the aqueous solutions of Co(II):3Cys and Co(III):3Cys were recorded on a Shimadzu UV-PC spectrophotometer in a 200–1000 nm range, using 1 and 0.01 mm quartz cells for the visible and UV regions, respectively.

Electron paramagnetic resonance

EPR spectra of Co(II):3Cys were recorded on a Brüker ER-200D X-band ESR spectrometer at 4.5 K because of the fast spin lattice relaxation time of Co(II). A 4 mm od quartz tube containing 80 μL of the investigated solution was put in an OXFORD helium flow cryostat and cooled down to 4.5 K. A $CoCl_2 \cdot 6H_2O$ solution was chosen as a reference. Computer-simulated EPR spectra were obtained using the following formula:[22]

$$S(\nu_c, B) = \sum_{\theta=0}^{\pi/2} \sum_{\phi=0}^{\pi/2} \sum_{M_I=-7/2}^{M_I=7/2} \langle g_1^2 \rangle f(\nu_c - \nu_0(B), \sigma_\nu) \Delta(\cos\theta) \Delta\phi$$

where $\langle {g_1}^2 \rangle$ is the powder-averaged transition probability, ν_c is the cavity resonance frequency and f the line shape function, assumed Gaussian or Lorentzian. The energy differences between energy levels $\nu_0(B)$ were evaluated using first-order perturbation theory. In the simulation, we assumed that the angular variation of the line width, σ_ν, has common principal axes with the g tensor. Dependence of the line width on microwave frequency and M_I due to random strain in frozen solutions was neglected, since a precise description of the ESR line width is not needed in this study.

Computational details

The $[Co(III)(Cys)_3]^{3-}$ structure (corresponding to the Co(III):3Cys experimentally studied system) was first obtained in vacuum by geometry optimization using DFT/BLYP calculations.[23] The 6-31 + + g(d,p) basis set was used for C, O, H, S and N atoms while for Co we used the (14s9p5d) primitive set of Wachters[24] supplemented with one s, two p and one d diffusive functions[25] and two f polarization functions,[26] the final contracted basis being [10s7p4d2f]. This basis set was recently used by one of us for the purpose of understanding

Co^{2+} binding to cysteine and selenocysteine,[27] providing a good agreement with results obtained with a larger basis.[28] Co(III) is a closed shell atom, while Co(II) is an open shell that was treated as a high-spin (quartet) state.

The geometry of least energy obtained from gas phase calculations was used as the starting point for DFT-based Car-Parrinello molecular dynamics (CPMD)[14] in water. Thus, the simulated system consists of one Co(III), 3 cysteine ligands entirely deprotonated due to the strong basic pH (each cysteine has a formal charge of −2) and 112 molecules of water. Water molecules were initially relaxed *via* classical molecular dynamics of pure water (125 water molecules) in a box having the same dimensions of the final simulation box (the box containing also the Co(III):3Cys complex). A cubic box of 15.52 Å length was used such that the pure water system used for the equilibration has a density of 1 g cm^{-3}. Then water molecules corresponding to the complex shape were removed and replaced by the complex obtained from in vacuum geometry optimisation. Thus CPMD simulation of the whole system was performed as previously described by one of us.[15b,28] The electronic structure of Co(III) is $[Ar]3d^6 4s^0$. Here we have used the same pseudo-potential as in our previous studies on Co(II),[15b] which only retains the $3d^6$ and $4s^0$ electronic levels as valence states. Here we report molecular dynamics simulations only of Co(III) that is closed shell atom, such that a restricted formalism was used.

CPMD simulations were done in the microcanonical NVE ensemble. Periodic boundary conditions were applied in order to mimic a bulk system with the Ewald summation technique to calculate the electrostatic interactions. The system was prepared at 300 K (initial velocities were chosen within a Boltzmann distribution centred on the desired temperature) and after an equilibration time of 1 ps the dynamics were propagated for 4 ps, strictly microcanonically. We used a fictitious electron mass of 400 au and a time step of 4 au (0.097 fs). Only the 4 ps equilibrium molecular dynamics were used for analysis. Car-Parrinello calculations were done with the CPMD code,[29] and gas phase energy minimization with the Gaussian03 package.[30]

X-Ray absorption spectroscopy

XAS data have been recorded at the BM29 beam line of the ESRF facility (Grenoble, France) as described previously.[20] For XANES, energy calibration was performed before and after the scan by recording a Co metallic foil. At 7700 eV the nominal energy resolution of the beamline is 0.7 eV. XANES normalization, EXAFS extraction and EXAFS fitting were carried out with the Athena and Artemis codes[31] as described previously.[20]

The EXAFS fitting procedure is based on scattering paths calculated from model clusters obtained by molecular dynamics calculation, each snapshot being truncated to 6 Å around the Co cation. This way, each snapshot leads to one model cluster in which the Co cation, its 3 cysteine ligands and about one layer of solvent water molecules are positioned at the centre of a sphere of 6 Å. Phases, amplitudes and electron mean free paths were calculated for each model cluster from each snapshot with Feff82 code.[32] In such a procedure, static and dynamical disorder (*i.e.* the apparent Debye–Waller factor) are implicitly included by taking in account several snapshots (*i.e.* several corresponding Feff calculations). A total of 10 clusters from 10 snapshots was necessary in order to obtain a satisfying fit. No Debye–Waller factor was therefore included in the fit by setting the exponential value to 1. The following paths from each Feff calculation were included in the fit: 3 × 10 Co–N and 3 × 10 Co–S single scattering paths; 3 × 10 Co–C(alpha N) and 3 × 10 Co–C(alpha S) single scattering paths; 3 × 10 Co–C–N and 3 × 10 Co–C–S triple scattering paths (each being doubly degenerate). The triple scattering paths were geometrically linked to the Co–S, N and Co–C(alpha S, N) paths. Finally, the floating parameters in the fit were: global amplitude parameters S_0, energy threshold e_0, Co–N distance R_N for the amino group, Co–S distance R_S for the thiol group and Co–C distance R_C for both carbons alpha to N and S in each cysteine ligand. All the 10 clusters were fitted together with linked global parameters (S_0 and e_0) and structural parameters R_N, R_S and R_C.

Results and discussion

Investigation of Co(III):3Cys

$[Co(III)(Cys)_3]^{3-}$ in solution exhibits a negative circular dichroism (CD) signal in the range of d–d transition (around 600 nm), characteristic of the Δ-*R,R,R-fac* diastereoisomer.[33] Therefore, the following structural investigation study will concern the Δ-*R,R,R-fac* configuration of $[Co(III)(Cys)_3]^{3-}$, noted more simply as Co(III):3Cys in the text.

Ligand field spectrophotometric absorptions of Co(III):3Cys occur at 442 and 570 nm in the visible region, corresponding to characteristic octahedral diamagnetic low spin Co(III) transitions, *i.e.* $[^1A_{1g} \rightarrow {}^1T_{2g}]$ and $[^1A_{1g} \rightarrow {}^1T_{1g}]$, respectively.[34] These data are in agreement with the literature, where UV-visible data are reported for the solid Co(III):3Cys complex.[21d,35] Co(III):3Cys exhibits an additional absorption band in the UV region at 273 nm, attributed to the sulfur-to-cobalt charge transfer (SCCT) band. In agreement with the literature,[36] this value suggests that the *cis*(*S*) isomer was formed, which was already assumed in our earlier work using EXAFS experiments.[20] XANES K edge features of cobalt complexes correspond to the formally 1s–4p transition in the dipolar approximation. The Co K edge spectrum of Co(III):3Cys exhibits the usual ''double'' white line (Fig. 1) as already described phenomenologically in our previous paper.[20] Pre-edge features of transition metals' K edges are attributed to transitions to the metal d orbitals (here 3d).[37] In the case of Co(III):3Cys, it is characteristic of cobalt in an octahedral or pseudo-octahedral symmetry because of its rather low intensity (compared to a high intensity pre-edge feature for tetrahedral complexes).[37]

In addition to our previous investigation of the local structure of the Co(III) cation, a combined molecular dynamics and EXAFS approach has been undertaken. It provides EXAFS data analysis with more reliable parameters for solution studies.[38] Structural models calculated by MD allow solvent effects to be accounted for in the calculation of the atomic potentials and avoid an arbitrary truncation of the

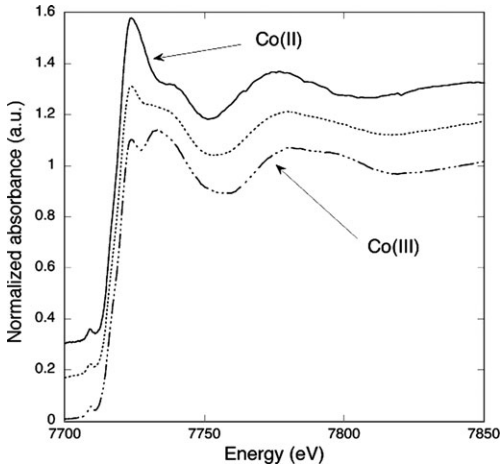

Fig. 1 XANES *in situ* monitoring of the oxidation of Co(II):3Cys (Co(II) in the graph) into Co(III):3Cys (Co(III) in the graph) at the Co K edge. An intermediate mixture of Co(II) and Co(III) is represented by the middle spectrum.

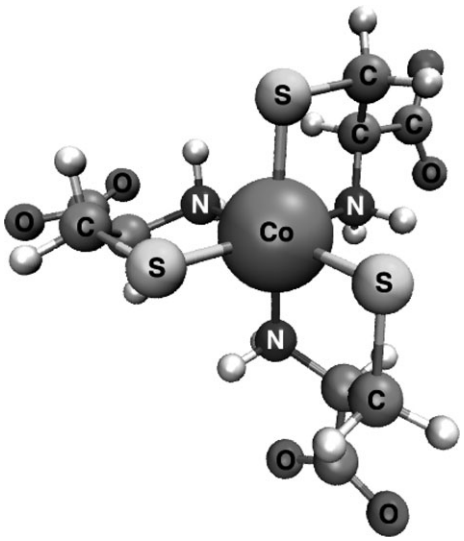

Fig. 2 Co(III):3Cys three-dimensional structure obtained from 0 K BLYP geometry optimization in the gas phase and used as starting structure in CPMD simulations in bulk water. H atoms are the small white atoms.

cluster (*cf.* experimental). It also accounts for structural stereochemical relaxation that can dramatically influence the cation coordination sphere in solution in comparison with solid state structures. Last, it allows dynamical effects to be partially accounted for, such as residence time of the ligands in the cation first coordination sphere or dynamical fluctuations of the geometry of the cation coordination sphere (*i.e.* dynamical disorder). In a classical fitting approach based on one rigid model cluster, these effects are accounted for by the well known Debye–Waller factor. Here, we have adopted another strategy that allows us to directly obtain Debye–Waller factors and reduce the number of fitted parameters. At this end, EXAFS data have been fitted using the modelled Co(III):3Cys structures obtained from Car-Parrinello molecular dynamics simulations.

MD simulations of the Co(III):3Cys complex have been produced in explicit water. The starting structure consisted of the optimised structure of Co(III):3Cys in vacuum (Fig. 2) and was subsequently surrounded by 112 water molecules, taking care that any hydrogen pointed towards S atoms at a distance less then 1.6 Å in the initial configuration. Thus, no solvent-to-solute proton transfer was spontaneously obtained during the simulation and a protonation state of the complex compatible with experimental pH conditions was kept during the simulation. In this way a stable simulation was obtained. Since no pH control was performed in our simulations, both carboxylic acid and thiol functions in each cysteine have been taken in the deprotonated state in order to be consistent with the basic pH of our experiments ($\approx$ 12) and the pK_a value of these acid functions (1.82 for carboxylic acid and 8.24 for thiol).[39] Note that here molecular dynamics is not aimed to investigate possible reactions with solvent, but only to point out structural and dynamical properties of the complex in its most stable protonation and conformational state at the given experimental conditions in the time length available from DFT based simulation.

In Fig. 3, we show the distance distribution of the atoms in the Co(III) first shell with the corresponding integrated values obtained from CPMD simulations. As expected, 3 N and 3 S are found in the Co(III) first coordination shell. Well-behaved "single peaked" distribution functions—where the width is a measure of structural disorder—are obtained. The overall arrangement of the cysteine ligands around the central cobalt atom is described by Co–X (where X = N, S, C(alpha S) and C(alpha N)) distances and Y–Co–Z angles (where Y, Z = N, S). Peaks of the distance distributions and average values, with relative fluctuations, obtained in water are presented in Table 1. The corresponding values obtained from gas phase geometry optimizations are also reported for comparison. Note that the solvation effect is remarkable on the Co–S distance which decreases from 2.38 Å in gas phase to 2.26 Å in solution and on the related Co–C(alpha S) distance, while other structural parameters are basically identical. This important modification in metal–ligand distance can be regarded as a typical solvation effect[40] that can be quantified by molecular dynamics still preserving information on solvent molecules' structural and dynamical behaviour. Water molecules are not in the first hydration shell of Co(III) but they hydrate the

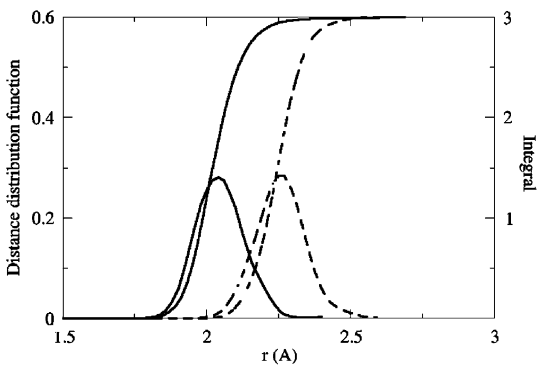

Fig. 3 Co–S and Co–N distance distribution functions obtained from $[Co(III):3Cys]_{aq}$ CPMD simulations.

Table 1 Structural parameters of Co(III):3Cys obtained from in vacuum 0 K energy minimization, $[Co(III):3Cys]_{vac}$, (in parentheses: geometry optimization in vacuum obtained by using a plane-waves/pseudo-potential representation) and Car-Parrinello molecular dynamics, $[Co(III):3Cys]_{aq}$. Maximum of distance (in Å) and angular (in °) distribution functions are reported for CPMD results, for which also averages with corresponding standard deviations are indicated in parentheses

	$[Co(III):3Cys]_{vac}$	$[Co(III):3Cys]_{aq}$
Co–S	2.38 (2.30)	2.26 (2.286 ± 0.097)
Co–N	2.01 (2.03)	2.04 (2.057 ± 0.082)
Co–C(alpha N)	3.01 (3.01)	3.02 (3.047 ± 0.091)
Co–C(alpha S)	3.22 (3.17)	3.12 (3.143 ± 0.095)
S–Co–S	93.0 (91.7)	89.25 (90.8 ± 4.9)
N–Co–N	94.1 (92.7)	90.75 (90.3 ± 4.2)
S–Co–N	86.5/177.3 (85.7/177.0)	87.2/174.3 (88.7 ± 4.9/172.8 ± 3.9)

overall complex, tuning structural and dynamical properties. The tris-cysteinato complex has two different H-bonding sites: the carboxylate and thiolate functions of the cysteine ligands. Each oxygen atom of the carboxylic group is hydrated *via* H-bonds that are dynamically formed and broken during the simulation: one H-bond is always present, while a second one is more labile. On the contrary, two static H-bonds are found on S atoms. More details on these and other solvation effects will be discussed elsewhere.[41]

Best fit EXAFS parameters obtained with MD model clusters for Co(III):3Cys are listed in Table 2 and fitted data (EXAFS and Fourier transform) are presented in Fig. 4. Although no additional Debye–Waller has been included in the fit, the two fits are of very good quality. In Table 2, best fit parameters obtained with the same adjustment procedure, but with the former EXAFS data of $[Co(III)Cys_3]^{3-}$, as described in our former paper,[20] are given for comparison. It is clearly observable that the structural parameters are in remarkably good agreement (within the error bar) with our previous results on the same complex,[20] where we used a traditional fitting procedure based on $[ZnCys_2]Na_2$ model compound. The second coordination shell is made of 3 carbon atoms alpha to the amino group and 3 carbon atoms alpha to the thiol group. During the fit, linking the carbon atom distances to the N and S distances based on a static geometry of the cysteine ligand did not lead to a satisfactory adjustment of the second shell contribution. Therefore both carbon distances were freed but linked together with the same parameter. The Co–C(alpha S) and Co–C(alpha N) distances are also reported in Table 2. They also compare well to the CPMD calculations within 0.03–0.04 Å agreement (Tables 1 and 2). From the above fitting method, Debye–Waller factors of the classical EXAFS formula (expressed as $\exp(-2\sigma_j^2k^2)$ where σ_j^2 is the Debye–Waller factor of the j scattering path) are implicitly included in the sum of the 10 snapshots. For single scattering paths, there is a clear relation between the std^2 (std = standard deviation) of the distance distribution function of neighbour j and σ_j^2. In this scheme, the std^2(Co–N) value of the Co–N distribution (0.0074 Å^2) is to be compared with the σ_j^2(Co–N) value of the classical EXAFS fitting (0.0049 Å^2) of our previous paper.[20] Also for the Co–S contribution: std^2(Co–S) = 0.0070 Å^2 and σ_j^2(Co–S) = 0.0052 Å^2. For both contributions, the std^2 value is overestimated by the same order (25%) compared to the Debye–Waller value. Taking into account the whole CPMD simulations, the variance of Co–S distance increases (std^2 = 0.0094 Å^2) while that of Co–N distance decreases a few (std^2 = 0.0067 Å^2). Note that std^2 obtained from CPMD simulations are obtained with the use of the BLYP functional. They represent a measure of molecular vibrations, and it is well known that CPMD/BLYP simulations provide overall vibrational spectra that are red-shifted generally about 100 cm^{-1} with respect to experimental ones mainly due to density functional softening.[42] Furthermore, in a recent study coupling EXAFS and CPMD simulations, we found that simulated disorder can be larger than fitted Debye–Waller factors by up to about 40% in the case of weak metal–solvent interactions.[28]

Investigation of Co(II):3Cys

The reaction of $Co(II)Cl_2 \cdot 6H_2O$ with an excess of cysteine under anaerobic conditions in basic medium leads to the formation of a blue purple complex in solution, Co(II):3Cys. To date, structural evidence for this complex is lacking although several efforts to acquire spectrophotometric data have been performed.[43] Hence, starting from the results of the different spectroscopic techniques that we have used, we are able to infer, as described below, what is the possible nature of the Co(II):3Cys complex.

UV-visible data of Co(II):3Cys are consistent with an octahedral high-spin d^7 Co(II) complex.[34] The transition observed

Table 2 Best fit parameters from the adjustments of the raw EXAFS spectra of Co(III):3Cys and Co(II):3Cys. The goodness of the fit is given by the *R* factor. Numbers of neighbours have been fixed. See the experimental for the fitting procedure

Contribution	3 Co–N std^2	3 Co–S std^2	3 Co–C(alpha N)	3 Co–C(alpha S)	Chi^2 (red) S_0, e_0
Co(II):3Cys	2.11(1) Å	2.37(1) Å	2.99(2) Å	3.12(2) Å	2
	0.0078 Å^2	0.0074 Å^2	0.0052 Å^2	0.0061 Å^2	0.6, 9.13
Co(III):3Cys	2.02(1) Å	2.26(1) Å	2.98(2) Å	3.09(2) Å	13
	0.0074 Å^2	0.0070 Å^2	0.0039 Å^2	0.0047 Å^2	0.7, 9.25
$[Co(III)(Cys)_3]^{3-}$ from ref. 20	2.01 Å	2.24 Å	2.96(2) Å	3.10(2) Å	24
	0.0049 Å^2	0.0052 Å^2	0.0046 Å^2	0.0063 Å^2	0.7, 9.25

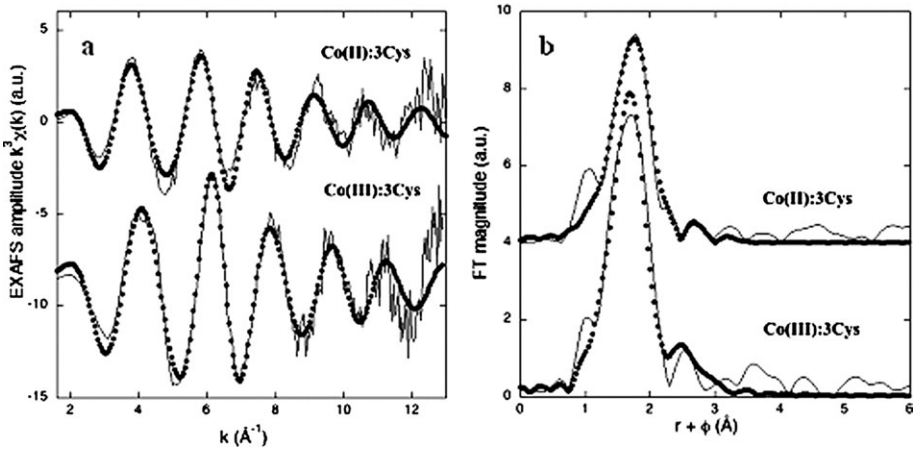

Fig. 4 Cobalt K edge raw EXAFS spectra (Fig. 4a) of complexes Co(II):3Cys and Co(III):3Cys and corresponding Fourier transforms (Fig. 4b). Fits are in dotted lines. For clarity, the EXAFS spectra and FT have been shifted in ordinates.

in the UV region (345 nm) is attributed to a SCCT band. The major d–d absorption band at 537 nm and a band with a weaker intensity at 695 nm are assigned to [$^4T_{1g}(F) \rightarrow {}^4T_{1g}(P)$] and [$^4T_{1g}(F) \rightarrow {}^4A_{2g}$] transitions, respectively. The EPR spectrum of a Co(II):3Cys solution under a nitrogen atmosphere at 4.5 K is shown in Fig. 5. This spectrum reveals an eight-line hyperfine structure, reflecting the coupling between a spin and a single ^{59}Co nucleus ($I = 7/2$, 100% abundant). The simulation of the experimental spectrum (spectrum b) was obtained by adding the individual contributions of two complexes: a narrow (A) (spectrum c) and very broad (B) (spectrum d). The large values of the line width for complex B suggest that some Co^{2+} ions experience a strong dipolar interaction, attributed to clusters that can be formed during the cooling and the freezing of the solution. Spin Hamiltonian parameters, deduced from the calculated spectrum (Table 3), and observed large g anisotropy are characteristic of high-spin Co(II) octahedral compounds ($S = 3/2$).[44] The sum of the three orthogonal g values of complexes A and B deviate from the trace of the cubic isotropic value.[22] This deviation is attributable to a strong distortion in the octahedral sites.[22] The existence of a distortion from a regular octahedral structure, which may be interpreted in terms of the Jahn–Teller

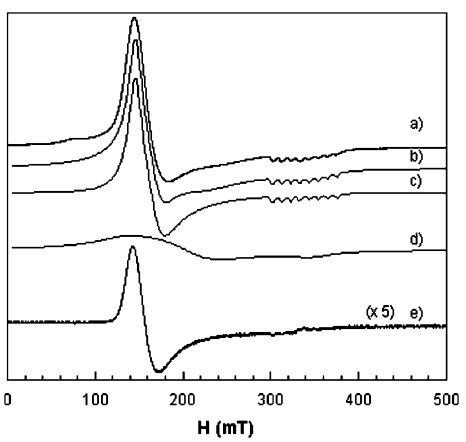

Fig. 5 EPR spectra of Co(II):3Cys recorded at 4.5 K. (a) Fresh solution, (b) simulation, (c) complex A, (d) complex B, (e) complex C.

effect, is usually encountered in high-spin Co(II) octahedral complexes.[45] On the contrary, low-spin Co(II) octahedral complexes are uncommon, since ligands tending to give a strong enough field to cause spin pairing involve the loss of ligands to form five- or four- rather than six-coordinate species.[45] Fig. 1 presents the Co K edge spectrum of Co(II):3Cys under an inert atmosphere. Qualitatively, it exhibits the usual feature of Co(II) compounds: an intense white line. The rather low intensity of the pre-edge peak also suggests that the cation lies in an octahedral or pseudo-octahedral geometry, confirming the results obtained from UV-visible and EPR spectroscopies. Due to the more atomic character of the final state of the pre-edge than of the edge, the oxidation state of Co is best characterized from the position of the pre-edge rather than from the edge.[20] A shift in the pre-edge to higher energy of 0.6 eV is observed here from Co(II):3Cys compared to Co(III):3Cys and corresponds to the 0.7 eV already reported.[20] Although this value is close from the energy resolution of the experiment, the resulting attribution of oxidation state confirms the EPR data, observable for Co(II) complexes due to their paramagnetic character. Co(II):3Cys and Co(III):3Cys adopt an octahedral geometry, justifying the use of the same model clusters for Co(II):3Cys to that used for Co(III):3Cys obtained from CPMD simulations. In this way, EXAFS data reveal that Co(II):3Cys is a mononuclear complex, in which the cobalt is coordinated to three S and three N atoms coming from the three cysteine ligands (Fig. 4). Averaged Co(II)–S and Co(II)–N distances were found to be 2.37(1) and 2.11(1) Å, respectively (Table 2), showing the expected lengthening in the donor atom–metallic centre bond when the oxidation state of the metallic cation decreases. Note that in Co(II) and Co(III) complexes the differences between the Co–N and Co–S distances are comparable (0.23 and 0.26 Å). First DFT calculations in the gas phase agree with the experimental picture providing a distorted cluster, with larger metal–donor bond lengths—the lengthening is $\sim$0.4 and $\sim$0.2 Å for Co–S and Co–N distances, respectively.

Studies on Co(II)-thiolate complexes of known structures are limited[46] and those relative to thiolate ligands containing additional N or O donor atoms are even more.[47] In the field of biochemistry, the coordination of Co(II)-thiolate complexes is

Table 3 Spin Hamiltonian parameters of Co(II) complexes in solution

	g_x	g_y	g_z	A_z/MHz	σ_x	σ_y	σ_z
Co(II) (A)	4.6 ± 0.1	4.0 ± 0.1	2.00 ± 0.01	146 ± 10	600 ± 50	300 ± 50	64 ± 5
Co(II) (B)	4.9 ± 0.5	3.3 ± 0.5	2.0 ± 0.1	—	3500 ± 500	2000 ± 500	800 ± 100
Co(II) (C)	4.7 ± 0.1	4.5 ± 0.1	2.0 ± 0.1	—	450 ± 50	440 ± 50	600 ± 50

dominated by the tendency to form tetrahedral units.[48] Co(II)–S distances encountered in these examples range between 2.23–2.33 Å[49] which are shorter than what we found for Co(II):3Cys, *i.e.* 2.37 Å. This difference may be attributed to the different environment of the metallic centres. To the best of our knowledge, apart from a few octahedral Co(II) complexes containing thioether ligands,[50] in which Co(II)–S bond lengths are obviously higher than 2.37 Å, only two examples related with a Co(II)-thiolate centre lying in an octahedral geometry are reported in the literature. They are in di- and tri-nuclear structures containing bridging and mixed bridging and terminal sulfurs, respectively.[20,51] The difference in the nuclearity in these complexes and the different role of the sulfur atom render difficult the comparison between the Co(II)–S distances. In the same way, octahedral complexes where Co(II) is bonded to nitrogen atoms coming from simple amino ligands are scarce, while N-donor atoms coming from pyridine,[52] Schiff bases[53] or urea derivatives[54] are reported in the literature. The Co(II)–N distances are different than that found in Co(II):3Cys due to the different nature of the N donor atom.

Monitoring of the oxidation of Co(II):3Cys into Co(III):3Cys

From the above combined spectroscopic and dynamical studies, the addition of four equivalents of cysteine on $Co(II)Cl_2 \cdot 6H_2O$ under an inert atmosphere yields a d^7 high-spin Co(II) complex in a distorted octahedral geometry. This complex, containing a chelating ligand incorporating a thiolate donor, is reported for the first time.

The synthesis of Co(III):3Cys can be carried out starting from a Co(III) precursor or from a Co(II) precursor. In this latter case, the interest is to monitor the oxidation of the metallic center by O_2 (eqn (1)).

$$4[Co(II):3Cys]^{4-} + O_2 + 2H_2O \rightarrow 4[Co(III):3Cys]^{3-} + 4OH^- \quad (1)$$

Upon exposure to air, the purple Co(II):3Cys becomes dark green, corresponding to the oxidation of Co(II) into Co(III). The monitoring of the oxidation using UV-vis spectroscopy shows shifts in absorbance bands toward the UV region. These changes are consistent with the formation of the Co(III):3Cys complex. XANES spectroscopy has been used to monitor changes in the oxidation state of cobalt (Fig. 1). Opening the sample holder to atmosphere leads to the progressive oxidation of Co(II) (middle spectrum) followed by its total oxidation to Co(III) as revealed by the differences in the edge features. A pronounced decrease in the intensity of the EPR signal is observed with the oxidation of Co(II) into Co(III), in agreement with the diamagnetic character of Co(III). The concomitant disappearance of the broad signal of complex B and the loss of hyperfine interaction have been also observed, while only the narrower signal remains (Fig. 5). The EPR parameters (Table 3) corresponding to the partially oxidized solution (C) show a small shift in the g_y value and the hyperfine interaction is no more resolved. These variations can be explained in terms of the slight differences in the distances and angles around the Co(II) centres in the coordination polyhedron upon the oxidation.

Conclusion

Although Co(III)-cysteinato complexes have been investigated using different spectroscopies for a long time, combination of CPMD simulations and XAS spectroscopy to assess structural details of Co(III):3Cys is reported for the first time. The very good agreement between the theoretical and experimental results show clearly the accuracy of the model provided by MD calculations. The same model cluster has been used to fit EXAFS data of Co(II):3Cys. The latter has been also characterized by XANES, EPR and UV-visible spectroscopies. To the best of our knowledge, Co(II):3Cys is the first octahedral Co(II)-thiolate complex containing additional N and O donor atoms thoroughly characterized in detail. In a last step, the monitoring of Co(II):3Cys oxidation by O_2 into Co(III):3Cys has been described using XANES, UV-vis and EPR spectroscopies.

The coupling of theoretical and experimental approaches is a promising tool for the study of transition metal complexes in solution, which is able to give insight to our understanding of the interaction of metallic ions with proteins at the molecular level. Moreover, stabilization of Co(II) species by bioligands such as amino acids and the monitoring of their oxidation by O_2, which are of major importance in living media, are likely to contribute to the evaluation of speciation and toxicity of cobalt compounds in biological systems. In this field, XANES experiments are more and more used as a tool to probe oxidation states of metallic ions in cells, providing information on their speciation.[55] Our results can be directly used as models, since cobalt complex references, particularly containing sulfur ligands, are needed to provide more useful comparisons with experimental spectra obtained from contaminated cells.

Acknowledgements

The authors want to thank N. Jamin and L. Bordes for CD measurements and Marie-Pierre Gaigeot for useful discussions. XAS measurements were carried out at European Synchrotron Radiation Facility for provision of synchrotron radiation facilities. This work was supported by Nuclear and Environmental Toxicology Program (DSV) and CEA/DEN/DDIN/MRTRA. The authors also thank CCRT (Centre de Calcul Recherche et Technologie, CEA) and IDRIS (CNRS Institut du Développement et des Ressources en Informatique

Scientifique) for generous access to their computational facilities.

References

1 J. J. R. Fausto da Silva and R. J. P. Williams, *The biological chemistry of the elements*, Clarendon Press, Oxford, 2nd edn, 2001.
2 R. H. Holm, P. Kennepohl and E. I. Salomon, *Chem. Rev*., 1996, **96**, 2239.
3 E. Farkas and I. Sovago, in *Amino Acids, Peptides and Proteins*, Royal Society of Chemistry, Cambridge, 2002, vol. 33, pp. 295–364.
4 (*a*) D. L. Nelson and M. M. Cox, *Lehninger principles of biochemistry*, Worth Publications, New York, 4th edn, 2004; (*b*) A. Sigel and H. Sigel, *Probing of proteins by metal ions and their low-molecular-weight complexes*, Marcel Dekker, New York, 2001, vol. 38.
5 (*a*) D. Lison, M. De Boeck, V. Verougstraete and M. Kirsch-Volders, *Occup. Environ. Med*., 2001, **58**, 619; (*b*) D. G. Barceloux, *J. Toxicol., Clin. Toxicol*., 1999, **37**(2), 201.
6 B. Le Guen and E. Ansoborlo, in *Le cobalt et ses isotopes*, Traité EMC: Elsevier SAS, Paris, 16-002-C-60, 2005.
7 (*a*) K. Popa, C. C. Pavel, N. Bilba and A. Cecal, *J. Radioanal. Nucl. Chem*., 2006, **269**(1), 155; (*b*) S. Szöke, G. Patzay and L. Weiser, *Desalination*, 2005, **175**, 179; (*c*) K. S. Leonard, D. McCubbin and B. R. Harvey, *J. Environ. Radioact*., 1993, **20**, 1.
8 C. Bresson, C. Lamouroux, C. Sandre, M. Tabarant, N. Gault, J. L. Poncy, J. L. Lefaix, C. Den Auwer, R. Spezia, M.-P. Gaigeot, E. Ansoborlo, S. Mounicou, A. Fraysse, G. Deves, T. Bacquart, H. Seznec, T. Pouthier, P. Moretto, R. Ortega, R. Lobinski and C. Moulin, *Biochimie*, 2006, **88**, 1619.
9 (*a*) I. Ascone, R. Fourme, S. S. Hasnain and K. Hodgson, *J. Synchrotron Radiat*., 2005, **12**, 1; (*b*) J. E. Penner-Hahn, *Coord. Chem. Rev*., 1999, **192**, 1101.
10 A. Levina, R. S. Armstrong and P. A. Lay, *Coord. Chem. Rev*., 2005, **249**(1–2), 141.
11 (*a*) M. Bühl and H. Kabrede, *J. Chem. Theor. Comput*., 2006, **2**, 1282; (*b*) L. Noodleman, T. Lovell, W.-G. Han, J. Li and F. Himo, *Chem. Rev*., 2004, **104**, 549.
12 G. Ferlat, J. Soetens, A. San Miguel and P. A. Bopp, *J. Phys.: Condens. Matter*, 2005, **17**(5), S145.
13 P. D'Angelo, V. Barone, G. Chillemi, N. Sanna, W. Mayer-Klaucke and N. V. Pavel, *J. Am. Chem. Soc*., 2002, **124**(9), 1958.
14 R. Car and M. Parrinello, *Phys. Rev. Lett*., 1985, **55**(22), 2471.
15 (*a*) I. Frank, M. Parrinello and A. Klamt, *J. Phys. Chem. A*, 1998, **102**(20), 3614; (*b*) R. Spezia, G. Tournois, J. Tortajada, T. Cartailler and M.-P. Gaigeot, *Phys. Chem. Chem. Phys*., 2006, **8**(17), 2040; (*c*) D. C. Marinica, G. Gregoire, C. Desfrancois, J. P. Schermann, D. Borgis and M.-P. Gaigeot, *J. Phys. Chem. A*, 2006, **110**(28), 8802.
16 (*a*) M. Sprik, J. Hutter and M. Parrinello, *J. Chem. Phys*., 1996, **105**(3), 1142; (*b*) P. L. Silvestrelli and M. Parrinello, *J. Chem. Phys*., 1999, **111**(8), 3572; (*c*) J. W. Handgraaf, E. J. Meijer and M.-P. Gaigeot, *J. Chem. Phys*., 2004, **121**(20), 10111.
17 (*a*) L. Rosso and M. E. Tuckerman, *Solid State Ionics*, 2003, **161**(3–4), 219; (*b*) V. Meregalli and M. Parrinello, *Solid State Commun*., 2001, **117**(7), 441.
18 (*a*) A. Dey, M. Chow, K. Taniguchi, P. Lugo-Mas, S. Davin, M. Maeda, J. A. Kovacs, M. Odaka, K. O. Hodgson, B. Hedman and E. I. Solomon, *J. Am. Chem. Soc*., 2006, **128**, 533; (*b*) C. Milsmann, A. Levina, H. H. Harris, G. J. Foran, P. Turner and P. A. Lay, *Inorg. Chem*., 2006, **45**, 4743; (*c*) V. Vrcek and M. Bühl, *Organometallics*, 2006, **25**, 358; (*d*) P. Vidossich and P. Carloni, *J. Phys. Chem. B*, 2006, **110**, 1437; (*e*) A. Dey, C. L. Roche, M. A. Walters, K. O. Hodgson, B. Hedman and E. I. Solomon, *Inorg. Chem*., 2005, **44**, 8349; (*f*) M. Bühl, *Inorg. Chem*., 2005, **44**, 6277; (*g*) M. Boero, M. Tateno, K. Terakura and A. Oshiyama, *J. Chem. Theor. Comput*., 2005, **1**, 925; (*h*) P. Maurer, A. Magistrato and U. Rothlisberger, *J. Phys. Chem. A*, 2004, **108**, 11494.
19 D. H. Baker and G. L. Czarnecki-Maulden, *J. Nutr*., 1987, **117**(6), 1003.
20 C. Bresson, S. Esnouf, C. Lamouroux, P. L. Solari and C. Den Auwer, *New J. Chem*., 2006, **30**, 416.
21 (*a*) A. P. Arnold and W. G. Jackson, *Inorg. Chem*., 1990, **29**, 3618; (*b*) R. D. Gillard and R. Maskill, *Chem. Commun*., 1968, (3), 160; (*c*) G. Gorin, J. E. Spessard, G. A. Wessler and J. P. Oliver, *J. Am. Chem. Soc*., 1959, **81**, 3193; (*d*) R. G. Neville and G. Gorin, *J. Am. Chem. Soc*., 1956, **78**, 4893.
22 J. R. Pilbrow, *Transition Ion Electron Paramagnetic Resonance*, Clarendon Press, Oxford, 1990.
23 (*a*) A. D. Becke, *Phys. Rev. A*, 1988, **38**(6), 3098; (*b*) C. Lee, W. Yang and R. G. Parr, *Phys. Rev. B*, 1988, **37**(2), 785.
24 A. J. H. Wachters, *J. Chem. Phys*., 1970, **52**, 1033.
25 P. I. Hay, *J. Chem. Phys*., 1977, **66**, 4377.
26 K. Raghavachari and G. W. Trucks, *J. Chem. Phys*., 1989, **91**, 1062.
27 R. Spezia, G. Tournois, T. Cartailler, J. Tortajada and Y. Jeanvoine, *J. Phys. Chem. A*, 2006, **110**, 9727.
28 R. Spezia, M. Duvail, P. Vitorge, T. Cartailler, J. Tortajada, G. Chillemi, P. D'Angelo and M.-P. Gaigeot, *J. Phys. Chem. A*, 2006, **110**, 13081.
29 J. Hutter, A. Alavi, T. Deutsch, M. Bernasconi, S. Goedecker, D. Marx, M. Tuckerman and M. Parrinello, *CPMD version 3.7.2*, IBM Research Division, IBM Corp and Max Planck Institute, Stuttgart.
30 M. J. Frisch, G. W. Trucks, H. B. Schlegel, G. E. Scuseria, M. A. Robb, J. R. Cheeseman, J. A. Montgomery, Jr., T. Vreven, K. N. Kudin, J. C. Burant, J. M. Millam, S. S. Iyengar, J. Tomasi, V. Barone, B. Mennucci, M. Cossi, G. Scalmani, N. Rega, G. A. Petersson, H. Nakatsuji, M. Hada, M. Ehara, K. Toyota, R. Fukuda, J. Hasegawa, M. Ishida, T. Nakajima, Y. Honda, O. Kitao, H. Nakai, M. Klene, X. Li, J. E. Knox, H. P. Hratchian, J. B. Cross, V. Bakken, C. Adamo, J. Jaramillo, R. Gomperts, R. E. Stratmann, O. Yazyev, A. J. Austin, R. Cammi, C. Pomelli, J. Ochterski, P. Y. Ayala, K. Morokuma, G. A. Voth, P. Salvador, J. J. Dannenberg, V. G. Zakrzewski, S. Dapprich, A. D. Daniels, M. C. Strain, O. Farkas, D. K. Malick, A. D. Rabuck, K. Raghavachari, J. B. Foresman, J. V. Ortiz, Q. Cui, A. G. Baboul, S. Clifford, J. Cioslowski, B. B. Stefanov, G. Liu, A. Liashenko, P. Piskorz, I. Komaromi, R. L. Martin, D. J. Fox, T. Keith, M. A. Al-Laham, C. Y. Peng, A. Nanayakkara, M. Challacombe, P. M. W. Gill, B. G. Johnson, W. Chen, M. W. Wong, C. Gonzalez and J. A. Pople, *GAUSSIAN 03*, Gaussian, Inc., Wallingford, CT, 2004.
31 B. Ravel and M. Newville, *J. Synchrotron Radiat*., 2005, **12**, 537.
32 J. J. Rehr and R. C. Albers, *Rev. Mod. Phys*., 2000, **72**, 621.
33 M. Kita and K. Yamanari, *J. Chem. Soc., Dalton Trans*., 1999, 1221.
34 A. B. P. Lever, *Inorganic Electronic Spectroscopy*, Elsevier, New York, 2nd edn, 1986.
35 M. Kita, K. Yamanari and Y. Shimura, *Bull. Chem. Soc. Jpn*., 1982, **55**, 2873.
36 T. Yonemura, Z. Bai, K. Okamoto, T. Ama, H. Kawaguchi, T. Yasui and J. Hidaka, *J. Chem. Soc., Dalton Trans*., 1999, 2151.
37 (*a*) J. E. Hahn, R. A. Scott, K. O. Hodgson, S. Doniach, S. R. Desjardins and E. I. Solomon, *Chem. Phys. Lett*., 1982, **88**(6), 595; (*b*) N. Kosugi, T. Yokoyama, K. Asakura and H. Kuroda, *Chem. Phys*., 1984, **91**(2), 249.
38 P. D'Angelo, O. M. Roscioni, G. Chillemi, S. Della Longa and M. Benfatto, *J. Am. Chem. Soc*., 2006, **128**(6), 1853.
39 P. Gockel, H. Vahrenkamp and A. D. Zuberbühler, *Helv. Chim. Acta*, 1993, **76**, 511.
40 (*a*) J. M. Martinez, R. R. Pappalardo and E. Sanchez Marcos, *J. Phys. Chem. A*, 1997, **101**, 4444; (*b*) J. M. Martinez, R. R. Pappalardo, E. Sanchez Marcos, B. Mennucci and J. Tomasi, *J. Phys. Chem. B*, 2002, **106**, 1118.
41 R. Spezia, C. Den Auwer, C. Bresson and M.-P. Gaigeot, in preparation.
42 M.-P. Gaigeot and M. Sprik, *J. Phys. Chem. B*, 2003, **107**, 10344.
43 (*a*) M. P. Schubert, *J. Am. Chem. Soc*., 1933, **55**, 3336; (*b*) B. J. McCormick and G. Gorin, *Inorg. Chem*., 1962, **1**, 691.
44 R. March, W. Clegg, R. A. Coxall, L. Cucurull-Sanchez, L. Lezama, T. Rojo and P. Gonzalez-Duarte, *Inorg. Chim. Acta*, 2003, **353**, 129.
45 F. A. Cotton and G. Wilkinson, *Advanced Inorganic Chemistry*, Wiley, New York, 5th edn, 1998.
46 I. G. Dance, *Polyhedron*, 1986, **5**, 1037.

47 (*a*) S. Chang, V. V. Karambelkar, R. D. Sommer, A. L. Rheingold and D. P. Goldberg, *Inorg. Chem.*, 2002, **41**, 239; (*b*) N. Duran, W. Clegg, L. Cucurull-Sanchez, R. A. Coxall, H. R. Jimenez, J.-M. Moratel, F. Lloret and P. Gonzalez-Duarte, *Inorg. Chem.*, 2000, **39**, 4821; (*c*) B. Kang, L. Weng, H. Liu, D. Wu, L. Huang, C. Lu, J. Cai, X. Chen and J. Lu, *Inorg. Chem.*, 1990, **29**, 4873.

48 (*a*) O. Y. Gavel, S. A. Bursakov, J. J. Calvete, G. N. George, J. J. G. Moura and I. Moura, *Biochemistry*, 1998, **37**, 16225; (*b*) I. Bertini, H. B. Gray, S. J. Lippard and J. S. Valentine, in *Bioinorganic Chemistry*, University Science Books, Sausalito CA, 1994; (*c*) G. Parkin, *Chem. Rev.*, 2004, **104**, 699; (*d*) A. K. Petros, S. E. Shaner, A. L. Costello, D. L. Tierney and B. R. Gibney, *Inorg. Chem.*, 2004, **43**, 4793.

49 (*a*) D. Maganas, S. S. Staniland, A. Grigoropoulos, F. White, S. Parsons, N. Roberston, P. Kyritsis and G. Pneumakakis, *Dalton Trans.*, 2006, 2301; (*b*) A. L. Nivorozhkin, B. M. Segal, K. B. Musgrave, S. A. Kates, B. Hedman, K. O. Hodgson and R. H. Holm, *Inorg. Chem.*, 2000, **39**, 2306; (*c*) C. Silvestru, R. Rösler, J. E. Drake, J. Yang, G. Espinosa-Perez and I. Haiduc, *J. Chem. Soc., Dalton Trans.*, 1998, 73; (*d*) T. Okamura, S. Takamizawa, N. Ueyama and A. Nakamura, *Inorg. Chem.*, 1998, **37**, 18.

50 (*a*) A. Grirrane, A. Pastor, E. Alvarez, C. Mealli, A. Ienco, D. Masi and A. Galindo, *Inorg. Chem. Commun.*, 2005, **8**, 463; (*b*) W. G. Haanstra, W. L. Driessen, M. Van Roon, A. L. E. Stoffels and J. Reedijk, *J. Chem. Soc., Dalton Trans.*, 1992, 481; (*c*) A. Mohamadou, C. Jubert and J.-P. Barbier, *Inorg. Chim. Acta*, 2006, **359**, 273.

51 T. Kotera, M. Fujita, H. Mikuriya, H. Tsutsumi and M. Handa, *Inorg. Chem. Commun.*, 2003, **6**, 322.

52 (*a*) W.-Z. Ju, R.-H. Jiao, P. Cao and R.-Q. Fang, *Acta Crystallogr., Sect. E: Struct. Rep. Online*, 2006, **E62**, m1012; (*b*) B. Zurowska, J. Mrozinski, Z. Ciunik and J. Ochocki, *J. Mol. Struct.*, 2006, **791**, 98; (*c*) P. I. Girginova, F. A. Almeida Paz, H. I. S. Nogueira, N. J. O. Silva, V. S. Amaral, J. Klinowski and T. Trindade, *Polyhedron*, 2005, **24**, 563; (*d*) R. March, W. Clegg, R. A. Coxall and P. Gonzalez-Duarte, *Inorg. Chim. Acta*, 2003, **346**, 87.

53 S. Sen, P. Talukder, S. K. Dey, S. Mitra, G. Rosair, D. L. Hughes, G. P. A. Yap, G. Pilet, V. Gramlich and T. Matsushita, *Dalton Trans.*, 2006, 1758.

54 M. Tiliakos, P. Cordopatis, A. Terzis, C. P. Raptopoulou, S. P. Perlepes and E. Manessi-Zoupa, *Polyhedron*, 2001, **20**, 2203.

55 (*a*) A. Levina, H. H. Harris and P. A. Lay, *J. Am. Chem. Soc.*, 2007, **129**(5), 1065; (*b*) P. D. Bonnitcha, M. D. Hall, C. K. Underwood, G. J. Foran, M. Zhang, P. J. Beale and T. W. Hambley, *J. Inorg. Biochem.*, 2006, **100**, 963; (*c*) M. D. Hall, G. J. Foran, M. Zhang, P. J. Beale and T. W. Hambley, *J. Am. Chem. Soc.*, 2003, **125**, 7524.